A Molecular [Mn$_{14}$] Coordination Cluster Featuring Two Slowly Relaxing Nanomagnets.

José Sánchez Costa,[a] Leoní A. Barrios,[a] Gavin A. Craig,[a] Simon J. Teat,[b] Fernando Luis,[c],* Olivier Roubeau,[c] Marco Evangelisti,[c] Agustín Camón [c] and Guillem Aromí [a],*

[a] Departament de Química Inorgànica, Universitat de Barcelona, Diagonal 647, 08028 Barcelona, Spain.

Fax: +34 934907725; E-mail: guillem.aromi@qi.ub.es.

[b] Advanced Light Source, Berkeley Laboratory, 1 Cyclotron Road, Berkeley, CA 94720, USA.

[c] Instituto de Ciencia de Materiales de Aragón, CSIC and Universidad de Zaragoza, Plaza San Francisco s/n, 50009, Zaragoza, Spain.

E-mail: fluis@unizar.es

ABSTRACT. Single molecule magnets (SMMs) could become the carriers of qubits in quantum computation. A major goal is the synthesis of molecules containing two well-defined SMMs. The use of a new polypyrazol ligand, H$_4$L, has enabled us to synthesize a cluster with SMM behavior containing two *quasi* independent, slowly relaxing [Mn$_7$] clusters. The dynamics of the magnetization within this species has been studied through ultra-low temperature magnetization and specific heat measurements. The later demonstrate that both cluster subunits of the molecule behave as anisotropic $S = 11/2$ spins.

Molecular nanomagnets occupy a central position among molecular materials that will shape the future of nanotechnology.[1] These species are coordination clusters of paramagnetic (3d and/or 4f) metals, exhibiting a range of spin states as a result of intramolecular magnetic exchange. Some of them feature large spin ground states and Ising-type zero-field splitting (ZFS), which confer them the potential of retaining the orientation of their molecular magnetic moment along the direction of the easy anisotropy axis. These molecules, now called single-molecule magnets (SMMs),[2, 3] have become suitable candidates to become qubits in quantum computation (QC).[4] In this regard, a key step was the demonstration that the tunnelling may be biased by the weak magnetic exchange between two SMMs within a supramolecular dimer,[5] which causes the quantum entanglement of the wave functions of both clusters, as demonstrated through HF-EPR.[6] Entanglement is of utmost relevance if spin clusters are to be considered as possible 2qubit quantum gates for the realization of QC.[7, 8] More recently, entanglement has been found between two fragments linked covalently within the same molecule, such as an Mn$_{12}$ ring described as two half-rings each with a $S = 7/2$ spin state,[9] or a Mn$_6$ cluster consisting of two $S = 6$ metal triangles. In these two cases, a weak ferromagnetic interaction couples both parts of the molecule. Stable molecular objects exhibiting such properties are much more interesting as potential quantum gates than supramolecular assemblies. However, *molecular* 'pairs of magnets' are hard to prepare by design and are thus extremely scarce, as compared with the large number and variety of reported SMMs,[10]

12 NBu$_4$MnO$_4$ + 58 Mn(AcO)$_2$·4H$_2$O + 40 H$_4$L + 30 MeOH →
5 [Mn$_{14}$O$_2$(OH)$_4$(OMe)$_4$(OAc)$_2$L$_2$(HL)$_4$(H$_2$L)$_2$(MeOH)$_2$(H$_2$O)$_6$]-
(AcO)$_2$ + 12 NBu$_4$AcO + 92 AcOH + 250 H$_2$O   (1)

more easily obtained by serendipity. Our group has been engaged

in the production of discrete coordination assemblies consisting in pairs of well-defined cluster nanomagnets, which we have termed 'molecular cluster pairs' (MCPs), as a promising strategy to access coordination chemistry-based 2qubit quantum gates. With this goal, ligands have been specifically designed to favour the aggregation of metals as two separate groups while maintaining them together within the same molecule,[11] or as a way to link two preformed clusters to each other.[12] We now report here the use of the ligand H$_4$L (2,6−bis(5−(2−hydroxyphenyl)−pyrazol−3−yl)−pyridine,[13] Scheme I) in a reaction with Mn ions, which promotes the aggreggation of paramgentic centers into two [Mn$_7$] clusters, while also ensuring that these are kept together within a molecular species. The product is a salt with formula [Mn$_{14}$O$_2$(OH)$_4$(OMe)$_4$(OAc)$_2$(L)$_2$(HL)$_4$(H$_2$L)$_2$(MeOH)$_2$(H$_2$O)$_6$]-(AcO)$_2$ (**1**) that contains a covalently linked pair of cluster nanomagnets; we also demonstrate in this paper that the slow relaxation of the magnetization of **1** is due to the individual properties of the [Mn$_7$] fragments, which amounts to having two SMMs within one molecular cation.
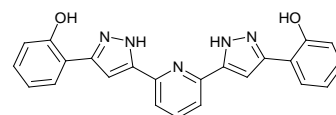

Scheme 1. H$_4$L.

Recent work has revealed that the product from reactions of H$_4$L with Mn(II)/Mn(III)/AcO$^-$ mixtures heavily depends on the solvent used, consisting of a [Mn$_4$] and a [Mn$_{10}$] cluster when using acetone or THF, respectively.[14] It was thus expected that a solvent with versatile coordination abilities would help to express further the structural diversity of the products resulting from this reaction system. Indeed, mixing NBu$_4$MnO$_4$, Mn(AcO)$_2$·4H$_2$O and H$_4$L (with 6:1:1.5 molar ratio) in MeOH led to crystals of **1** after layering the resulting dark brown solution with Et$_2$O. This product is drastically different from the clusters previously characterized, although with some common local structural features (see below) and incorporates bridging methoxide groups. In this reaction the comproportionation between Mn(VII) and Mn(II) is exploited to facilitate the formation of a majority of Mn(III) ions. Likewise, the oxide ions liberated from MnO$_4^-$ furnish the necessary base for the (partial) deprotonation of H$_4$L and some molecules of MeOH. A balanced reaction for the formation of **1** may
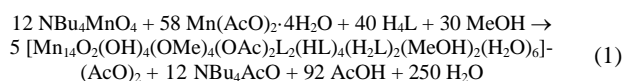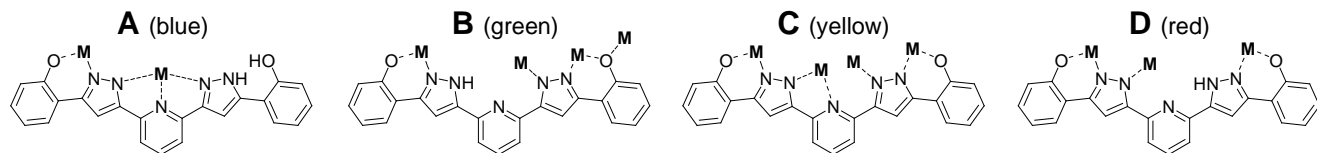
Scheme 2. Coordination modes exhibited by the H_4L-based ligands in **1**.

be written (eq. 1), although it is clear that other chemical processes also take place in solution, not unveiled in the solid phase.

Compound **1** is a salt of two AcO^- anions and a $[Mn_{14}]^{2+}$ complex cation (Fig. 1). The latter is a coordination cluster of fourteen Mn(II/III) ions distributed into two well differentiated and symmetry related groups of seven metals. Within each $[Mn_7]$ fragment, the donors of four distinct, partially deprotonated H_4L ligands (see Scheme II for coordination modes) keep the metals together, indirectly through the ligand backbone structure, and directly by means of four $-N-N-$ (from pyrazolyl moieties) and one $\mu-O$ (phenolate based) bridges. In addition there are one μ_3-O^{2-} (O13), one μ_3-OH^- (O10), one $\mu-OH^-$ (O17), two $\mu-MeO^-$ and one $\mu-AcO^-$ (*syn,syn*) ligands helping to cement the metals of the aggregate. The coordination is also achieved by three H_2O, one MeOH and five phenolate terminal groups, each of the latter associated to a bridging pyrazolyl moiety (see above) in the establishment of six-member chelate rings. Finally, one of the HL^{3-} groups of the $[Mn_7]$ fragment reaches out to the other heptanuclear aggregate, chelating one metal of the latter (Mn7) through a phenolate/p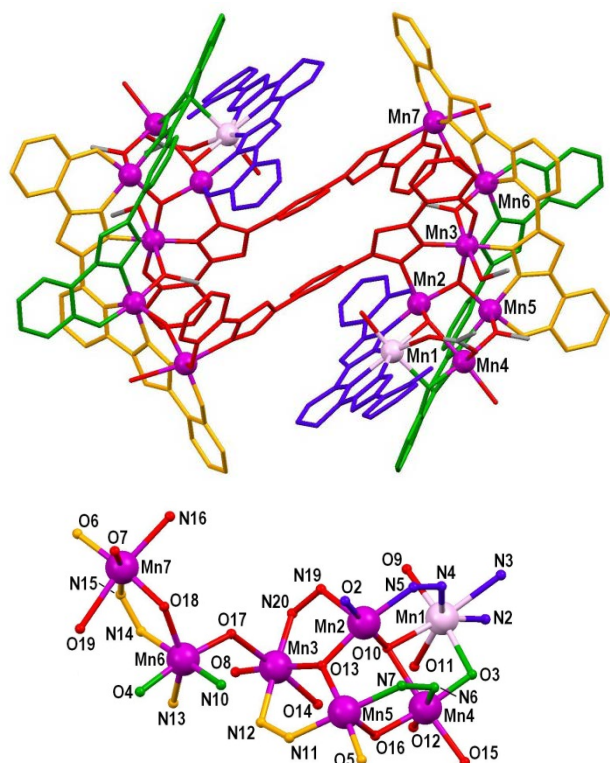yrazolyl fragment, thus completing a double long-distance link between both well-defined clusters of the molecule. The metal topology within each aggregate (Fig. 1, bottom) may be described as a puckered pentagon in form of capped square, linked through the "capping" metal to a Mn_2 metal pair acting as a "tail". It contains six Mn ions in the oxidation state +3 and one in the oxidation state +2 (Mn1). This assignment was decided on the basis of BVS, charge balance considerations and the metric parameters and coordination geometries around the metal ions. Indeed, Mn3 to Mn7 exhibit Jahn-Teller elongated (distorted) coordination geometries, while Mn2 exhibits axially elongated square pyramidal coordination. All H_2O and MeOH molecules occupy axial sites, the rest of these positions being occupied by pyridyl or pyrazolyl moieties, μ_3-OH^-, $\mu-OH^-$ or $\mu-MeO^-$ (the latter two in very distorted situations, corresponding to Mn6 to O18 and Mn5 to O16, respectively). Low valent Mn1 is in a distorted pentagonal bipyramidal geometry. The structure of the complex in **1** underscores the dual function that H_4L may play in its various deprotonated forms. First, it is a highly versatile donor, here exhibiting four different coordination modes (Scheme II), none of which coincident with the four previously observed.[13, 14] This confers to the ligand the ability to form metal aggregates with a large variety of structures. On the other hand, the presence of two groups of donor atoms separated by a spacer that not always coordinates (in **1** it does for only half of the ligands) adds the potential of linking covalently two distant entities, as revealed here with the formation of the first MCP with H_4L. The cation of **1** is only the eighth $[Mn_{14}]$ cluster reported, since the first example was published in 2002[15] (full list of references in the SI).

Variable temperature bulk magnetic susceptibility measurements (from 2 to 300 K) show the presence of exchange coupling
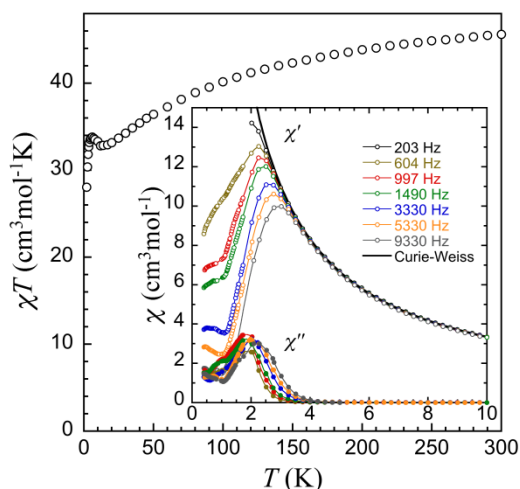

Figure 1. (top) Structure of the complex cation of **1** $[Mn_{14}O_2(OH)_4(OMe)_4(OAc)_2(L)_2(HL)_4(H_2L)_2(MeOH)_2(H_2O)_6]^{2+}$, with each crystallographic type of deprotonated H_4L ligand in a different color. For the rest of ligands, red is O and grey is C. H atoms not shown. Only unique Mn atoms labelled. (bottom) Labelled representation of the core of each $[Mn_7]$ fragment in **1**. Darker Mn ions are +3 and lighter are +2.

Figure 2. Plot of $\chi_M T$ *vs* T for complex **1**. Inset: plots of AC χ' (full symbols) and χ'' (open symbols) *vs* T per mol of **1**. The solid line is a Curie-Weiss fit of the 223 Hz data in the 3 to 10 K range (see text for details).

between the spins of the Mn ions within the cluster of **1**. The results in form of a $\chi_M T$ *vs* T plot (Fig 2, χ_M is the molar para-magnetic susceptibility) indicate a combination of ferro- and antiferromagnetic interactions. In cooling from 300 K to 14 K, $\chi_M T$ decreases from 45.6 cm^{3}Kmol^{-1} down to 32.8 cm^{3}Kmol^{-1}. This minimum is followed by a maximum of 33.8 cm^{3}Kmol^{-1} at 6 K and finally, $\chi_M T$ reaches 28.0 cm^{3}Kmol^{-1} at 2 K. These data suggest the presence of a high molecular spin ground state. Further insights into this ground state were obtained through AC susceptibility measurements, shown in the inset of Fig. 2. Between 3 and 10 K, the equilibrium susceptibility χ_T can be determined from measurements performed at sufficiently low frequencies (223 Hz in this experiment). It obeys the Curie-Weiss law $\chi' = C/(T-\theta)$ with $C = 33.8$ cm^{3}Kmol^{-1} and $\theta = -0.066$ K (Fig. S1). The Curie constant is compatible[16] with either a total $S = 15/2$ ground state for the whole molecule, or with two $S = 11/2$ spins embodied inside the cluster, both with $g = 2$. The isothermal ($T = 2$ K) magnetization clearly favours the scenario of two quasi-independent $S = 11/2$ units in the molecule of **1** (Fig. S2).

The goal of performing coherent manipulation of molecular spins, as is necessary for applications in QC, underscores the importance of understanding the magnetic relaxation mechanisms. Relaxation times, τ, can be obtained by varying the frequency of the AC susceptibility experiments. Data measured down to 400 mK reveal the existence of frequency dependent maxima in the χ' and χ'' *vs* T plots (χ' and χ'' are the in-phase and out-of-phase components of the dynamical susceptibility, respectively; Fig. 2, inset). The results confirm that **1** exhibits the slow relaxation of the magnetization that is typical of SMMs. As a first approximation, the maxima of the χ'' *vs* T plots correspond to the condition $\tau = 1/\omega$. The relaxation times derived from this relation follow the Arrhenius law (Eq. 2, Fig. 3) with an activation energy $U/k_B = 18(1)$ K and a pre-exponential factor $\tau_0 = 4(2) \times 10^{-9}$ s.

$$\frac{1}{\omega} = \tau_0 e^{\left(U/k_B T\right)} \tag{2}$$

This behavior reveals that the spins flip *via* a thermally activated mechanism over the magnetic anisotropy barrier. For the simplest Hamiltonian for the isolated ground state with uniaxial anisotropy, $H = DS_z^2$, the energy barrier for a non-integer spin ground state reads $U = (S_z^2 - \frac{1}{4}) \times |D|$. Using the activation energy determined from the Arrhenius fit gives $D/k_B = 0.6$ K each of the two $S = 11/2$ entities. Additional information on the relaxation of these spins was obtained from the dependence of χ' and χ'' on frequency at 2 K, which can be described by the Cole-Cole functions (eqs. 3 and 4).

$$\chi' = \chi_S + (\chi_T - \chi_S)\frac{1 + (\omega\tau)^\beta \cos\left(\frac{\pi}{2}\beta\right)}{\left[1 + (\omega\tau)^\beta \cos\left(\frac{\pi}{2}\beta\right)\right]^2 + \left[(\omega\tau)^\beta \sin\left(\frac{\pi}{2}\beta\right)\right]^2} \tag{3}$$

$$\chi'' = (\chi_T - \chi_S)\frac{(\omega\tau)^\beta \sin\left(\frac{\pi}{2}\beta\right)}{\left[1 + (\omega\tau)^\beta \cos\left(\frac{\pi}{2}\beta\right)\right]^2 + \left[(\omega\tau)^\beta \sin\left(\frac{\pi}{2}\beta\right)\right]^2} \tag{4}$$

In these equations, χ_S and χ_T are the adiabatic (infinite frequency) and isothermal (equilibrium) susceptibility limits, respectively, and the parameter β gives a measure of the distribution of relaxation times within the system (with $\beta = 1$ for a single relaxation process). By fitting both components of the susceptibility with these equations (Fig. S3) we find $\chi_S = 1.66$ cm^{3}mol^{-1} and $\beta = 0.53$. The fact that $\beta < 1$, indicating a broad dispersion of τ's, may be due to a distribution of anisotropy parameters or to the presence of various relaxation channels, e.g. associated with close lying excited spin states. The value of χ_S provides access to an

independent estimation of D as extracted from eq. 5,[16] which applies to two spin subunits within the same molecule. This calculation affords $D/k_B = 0.57$ K, in remarkable agreement with the value obtained from the Arrhenius plot.

$$\chi_S = \frac{4N_A g^2 \mu_B^2 S}{3(2S-1)D} \tag{5}$$

The dependence of τ with temperature (from ca 2.7 to 1 K) was determined by fitting the χ' *vs* T data measured at $\nu = 3330$ Hz with the first of Cole-Cole equations (see above). The number of free parameters was reduced by setting β and χ_S equal to the values determined at 2 K, and $\chi_T = C/(T - \theta)$. The data obtained by this method agree very well with the relaxation time values extracted from the maxima of the χ'' *vs* T plots (Arrhenius plot, Fig. 3). Below approximately 1.5 K, τ begins to deviate from the Arrhenius law, thus departing from the pure thermally activated relaxation. The additional data point obtained from C_p *vs* T measurements (see below) confirms this trend, while also indicating that a quantum relaxation mechanism is not yet dominant at 0.7 K. Nonetheless, the isothermal magnetization measured on single crystals at temperatures from 0.2 K to 2 K (Fig. 4) shows hysteresis loops below 1.2 K, confirming the SMM behaviour in **1**. The loops widen as T decreases and are smooth, with no clear traces of the steps characteristic of resonant quantum tunnelling within SMMs.

An independent confirmation of this puzzling behavior was obtained from AC susceptibility measurements performed under
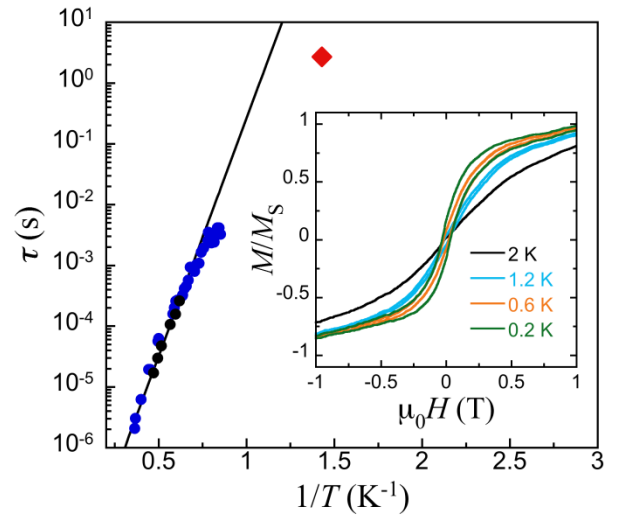

Figure 3. Plot of τ *vs* $1/T$ for complex **1** extracted from the maxima of χ'' *vs* T at different frequencies (black circles), from χ' *vs* T data at $\nu = 3330$ Hz using the Cole-Cole equations and the parameters from the Cole-Cole fits (blue circles) and from C_p *vs* T (red rhomb). The solid line is a least squares Arrhenius fit, valid above 1.8 K. Inset: Magnetization hysteresis loops at various constant temperatures for a single-crystal of **1**.

finite DC magnetic fields. At $T = 2$ K (Fig. S4), the results show a smooth decline of χ' and χ'' upon the increase of the magnetic field, with no indication of the resonant behavior seen in many SMMs.[17, 18] This observation becomes even more evident when examining the magnetic field dependence of the relaxation time, τ (Fig. S5), which was obtained from the susceptibility measurements at 2 K using Cole-Cole fits (eqs. 3 and 4). The results show that τ is maximum at $H = 0$, in striking contrast with the pronounced minimum observed for SMMs flipping their spins *via* quantum tunnelling. The field dependence of τ resembles instead that expected for classical spins. This classical response might be due in part to the presence of an exchange field between the [Mn$_7$] sub-units acting as an effective bias that energetically detunes the spin-up and spin-down states, as previously observed with a su-

pramolecular pair of [Mn$_4$] SMMs.[5]

Additional support for the presence of two quasi-isolated [Mn$_7$] units in the cluster of **1** was obtained from specific heat capacity measurements in the 20–0.4 K temperature range. Figure 4 shows data measured in zero field and under constant magnetic fields of 0.5 and 1 T. Down to 0.7 K, the zero-field data are satisfactorily reproduced by simply considering the ZFS of two $S = 11/2$ spins with $D/k_B = 0.6$ K and a lattice heat capacity made by the sum of an Einstein and a Debye ($\theta_D = 10$ K) contributions. Considering a single $S = 15/2$ spin does not allow to reproduce the experimental hump centered at ca. 2 K, thus clearly confirming the presence of two [Mn$_7$] moieties with spin ground-state $S = 11/2$. Moreover,
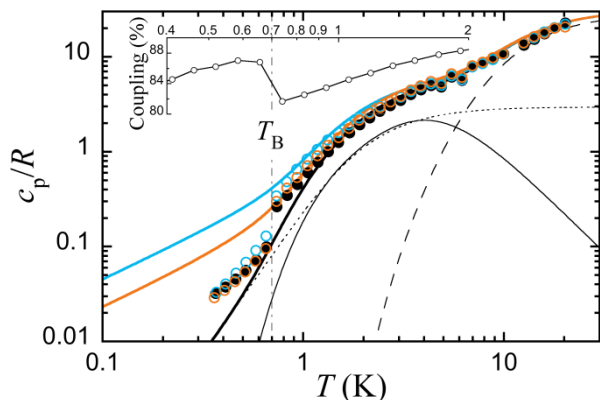

Figure 4. Heat capacity of **1** in zero-field (black full circles) and under 0.5 and 1 T (open blue and orange circles, respectively). Full lines are the computed heat capacity considering the ZFS of two $S = 11/2$ spins with $D/k_B = 0.6$ K (full thin line), plus Debye (dotted line) and Einstein (dashed line) contributions to the lattice heat capacity. The inset shows the minimum exhibited at 0.7 K by the thermal coupling parameter of the PPMS, and indicative of the blocking temperature T_B of the slow relaxing species in **1**.

the data measured under an applied magnetic field are also well reproduced by the same model. Interestingly, the C_p *vs. T* data also provide additional evidence for the superparamagnetic blocking of the SMM units in **1**. As it has been observed in other anisotropic clusters, like Mn$_{12}$,[17] Fe$_8$,[17, 19] and Mn$_4$,[20] a clear jump is detected at $T = 0.7$ K, accompanied by a steep minimum in the thermal coupling parameter that measures the exponential character of the temperature relaxation. The departure from the standard single-exponential decay is related to the fact that, close to the blocking temperature T_B, the heat capacity depends on the measurement time-scale.[17] The τ value derived from these data is included in Figure 3, together with the data derived from the AC magnetic susceptibility. Due to the superparamagnetic blocking, no clear signature of the intramolecular exchange coupling between the two [Mn$_7$] units can be obtained from the heat capacity data. Nevertheless, hints of a weak coupling are given by the τ *vs. H* data (see above), the non-zero value of χ'' observed down to the lowest temperatures, the excess heat capacity observed below 1 K, or the absence of a purely quantum tunneling relaxation regime.

In conclusion, the complex salt [Mn$_{14}$O$_2$(OH)$_4$(OMe)$_4$(OAc)$_2$(L)$_2$(HL)$_4$(H$_2$L)$_2$(MeOH)$_2$(H$_2$O)$_6$]-(AcO)$_2$ (**1**) has been formed thanks to the dual function of ligand H$_4$L (in various deprotonated forms); *i*) facilitating the aggregation of Mn ions into high spin clusters and *ii*) bridging two of these fragments within one molecule. One major goal in the pursuit of using SMMs for QC is the ability to connect them as identifiable entities within stable molecular assemblies. The slow relaxing nature of the magnetization of both [Mn$_7$] units included in **1** has been demonstrated and described by ultralow temperature experiments, as well as its dynamic behavior. The dynamic properties of both units are influenced by the exchange between both halves of the molecular cluster, as was demonstrated for the first time with pairs of SMMs connected in the crystal *via* supramolecular interactions.

Supporting Information Available: Complete experimental details (PDF). X-ray crystallographic files (CIF). These materials are available free of charge via the Internet at http://pubs.acs.org.

REFERENCES.

[1] R. E. P. Winpenny, E. J. L. McInnes, Molecular Nanomagnets, John Wiley & Sons, Ltd, 2010.

[2] D. N. Hendrickson, G. Christou, H. Ishimoto, J. Yoo, E. K. Brechin, A. Yamaguchi, E. M. Rumberger, S. M. J. Aubin, Z. M. Sun, G. Aromí, Polyhedron 2001, 20, 1479-1488.

[3] R. Sessoli, H. L. Tsai, A. R. Schake, S. Y. Wang, J. B. Vincent, K. Folting, D. Gatteschi, G. Christou, D. N. Hendrickson, J. Am. Chem. Soc. 1993, 115, 1804-1816.

[4] M. N. Leuenberger, D. Loss, Nature 2001, 410, 789-793.

[5] W. Wernsdorfer, N. Aliaga-Alcalde, D. N. Hendrickson, G. Christou, Nature 2002, 416, 406-409.

[6] S. Hill, R. S. Edwards, N. Aliaga-Alcalde, G. Christou, Science 2003, 302, 1015-1018.

[7] G. A. Timco, T. B. Faust, F. Tuna, R. E. P. Winpenny, Chem. Soc. Rev. 2011, DOI: 10.1039/C1030CS00151A.

[8] F. Troiani, M. Affronte, Chem. Soc. Rev. 2011, DOI: 10.1039/c1030cs00158a.

[9] C. M. Ramsey, E. Del Barco, S. Hill, S. J. Shah, C. C. Beedle, D. N. Hendrickson, Nat. Phys. 2008, 4, 277-281.

[10] G. Aromí, E. K. Brechin, Struct. Bond. 2006, 122, 1-67.

[11] L. A. Barrios, D. Aguilà, O. Roubeau, P. Gamez, J. Ribas-Ariño, S. J. Teat, G. Aromí, Chem.-Eur. J. 2009, 15, 11235-11243.

[12] E. C. Sañudo, T. Cauchy, E. Ruiz, R. H. Laye, O. Roubeau, S. J. Teat, G. Aromí, Inorg. Chem. 2007, 46, 9045-9047.

[13] G. A. Craig, L. A. Barrios, J. S. Costa, O. Roubeau, E. Ruiz, S. J. Teat, C. C. Wilson, L. Thomas, G. Aromí, Dalton Trans. 2010, 39, 4874-4881.

[14] J. Sánchez-Costa, G. A. Craig, L. A. Barrios, O. Roubeau, E. Ruiz, S. Gómez-Coca, S. J. Teat, G. Aromí, Chem., Eur. J. 2011, 17, 4960 – 4963.

[15] G. Aromí, A. Bell, S. J. Teat, A. G. Whittaker, R. E. P. Winpenny, Chem. Commun. 2002, 1896-1897.

[16] J. L. Garcia-Palacios, J. B. Gong, F. Luis, J. Phys.-Condes. Matter 2009, 21, 456006.

[17] F. L. Mettes, F. Luis, L. J. de Jongh, Phys. Rev. B 2001, 64, 17.

[18] J. M. Hernández, X. X. Zhang, F. Luis, J. Bartolome, J. Tejada, R. Ziolo, Europhys. Lett. 1996, 35, 301-306.

[19] M. Evangelisti, F. Luis, F. L. Mettes, R. Sessoli, L. J. de Jongh, Phys. Rev. Lett. 2005, 95, 4.

[20] M. Evangelisti, F. Luis, F. L. Mettes, N. Aliaga, G. Aromí, J. J. Alonso, G. Christou, L. J. de Jongh, Phys. Rev. Lett. 2004, 93, 4.